

Multimodal Imaging in Rats Reveals Impaired Neurovascular Coupling in Sustained Hypertension

Novella Calcinaghi, PhD; Matthias T. Wyss, MD, PhD*; Renaud Jolivet, PhD*; Anand Singh, MSc; Anna L. Keller, PhD; Stephan Winnik, MD; Jean-Marc Fritschy, PhD; Alfred Buck, MD, MSc; Christian M. Matter, MD; Bruno Weber, PhD

Background and Purpose—Arterial hypertension is an important risk factor for cerebrovascular diseases, such as transient ischemic attacks or stroke, and represents a major global health issue. The effects of hypertension on cerebral blood flow, particularly at the microvascular level, remain unknown.

Methods—Using the spontaneously hypertensive rat (SHR) model, we examined cortical hemodynamic responses on whisker stimulation applying a multimodal imaging approach (multiwavelength spectroscopy, laser speckle imaging, and 2-photon microscopy). We assessed the effects of hypertension in 10-, 20-, and 40-week-old male SHRs and age-matched male Wistar Kyoto rats (CTRL) on hemodynamic responses, histology, and biochemical parameters. In 40-week-old animals, losartan or verapamil was administered for 10 weeks to test the reversibility of hypertension-induced impairments.

Results—Increased arterial blood pressure was associated with a progressive impairment in functional hyperemia in 20- and 40-week-old SHRs; baseline capillary red blood cell velocity was increased in 40-week-old SHRs compared with age-matched CTRLs. Antihypertensive treatment reduced baseline capillary cerebral blood flow almost to CTRL values, whereas functional hyperemic signals did not improve after 10 weeks of drug therapy. Structural analyses of the microvascular network revealed no differences between normo- and hypertensive animals, whereas expression analyses of cerebral lysates showed signs of increased oxidative stress and signs of impaired endothelial homeostasis upon early hypertension.

Conclusions—Impaired neurovascular coupling in the SHR evolves upon sustained hypertension. Antihypertensive monotherapy using verapamil or losartan is not sufficient to abolish this functional impairment. These deficits in neurovascular coupling in response to sustained hypertension might contribute to accelerate progression of neurodegenerative diseases in chronic hypertension. (*Stroke*. 2013;44:1957-1964.)

Key Words: cerebrovascular circulation ■ hypertension ■ multimodality imaging ■ neurovascular coupling ■ spontaneously hypertensive rats

The sequelae of arterial hypertension (aHTN) account for more than one third of deaths in Western countries.¹ It constitutes one of the major risk factors for hemorrhagic stroke² and may be a leading cause of cognitive impairment.³

The effects of aHTN on brain hemodynamics have been investigated in several animal studies yielding contradictory results. These may depend on strains, anesthetic conditions, and whether the study assessed evoked signals or resting conditions. For instance, resting cerebral blood flow (CBF) in spontaneously hypertensive rats (SHR) has been reported

to be similar to,^{4,5} less than,⁶ or greater than⁷ that of controls (Wistar Kyoto rats). In another model where aHTN was induced by systemic injection of angiotensin II,^{8–10} CBF responses evoked by whisker stimulation were reduced in hypertensive mice in comparison with normotensive animals. In human positron emission tomography studies, aHTN seems to induce a mild dampening in regional CBF (rCBF) response during memory tasks that is more pronounced in frontal and subcortical regions.¹¹

The prevalence of aHTN increases with age, which may also affect CBF and neurovascular coupling (NVC). In human

Received November 19, 2012; final revision received April 5, 2013; accepted April 8, 2013.

From the Institute of Pharmacology and Toxicology (N.C., M.T.W., R.J., A.S., J.-M.F., B.W.), Cardiovascular Research, Institute of Physiology (S.W., C.M.M.), University of Zurich, Zurich, Switzerland; Neuroscience Center Zurich, University of Zurich and Swiss Federal Institute of Technology (ETH) Zurich, Zurich, Switzerland (N.C., M.T.W., R.J., A.S., J.-M.F., A.B., B.W.); Zurich Center for Integrative Human Physiology (ZIHP), University of Zurich, Zurich, Switzerland (N.C., M.T.W., A.B., C.M.M., B.W.); Max Planck Institute for Biological Cybernetics, Tübingen, Germany (A.L.K.); and Divisions of Nuclear Medicine (A.B.) and Cardiology (S.W., C.M.M.), PET Center, University Hospital Zurich, Zurich, Switzerland.

*Drs Wyss and Jolivet contributed equally to this article.

The online-only Data Supplement is available with this article at <http://stroke.ahajournals.org/lookup/suppl/doi:10.1161/STROKEAHA.111.000185/-/DC1>.

Correspondence to Bruno Weber, PhD, Institute of Pharmacology and Toxicology, University of Zurich, Rämistrasse 100, CH-8091 Zürich, Switzerland. E-mail bweber@pharma.uzh.ch

© 2013 American Heart Association, Inc.

Stroke is available at <http://stroke.ahajournals.org>

DOI: 10.1161/STROKEAHA.111.000185

positron emission tomography studies, aging is usually associated with a significant decrease in resting CBF.¹² In addition, aging is accompanied by a reduction in the blood oxygenation level-dependent response.¹³ Similarly, Dubeau et al¹⁴ have recently reported a reduced hemodynamic response in the somatosensory cortex of aged rats (24 and 40 months) with unaltered metabolic rate of oxygen use.

In the present study, using a multimodal brain imaging approach, we investigated the effects of sustained aHTN of variable duration on the hemodynamics and structure of the somatosensory cortex in SHR, a model of essential genetic aHTN. In a second phase, we examined the reversibility of alterations by antihypertensive treatment using either losartan or verapamil. To the best of our knowledge, there is no prior study investigating the impact of sustained increased arterial blood pressure on cerebral hemodynamics using a combination of methods ranging from microvascular 2-photon microscopy to widefield intrinsic optical imaging.

Methods

Animals

All experimental procedures were reviewed and approved by the local ethical committee and the cantonal veterinary authority. They conform to the guidelines of the Swiss Animal Protection Law, Veterinary Office, Canton Zurich. The animals were kept in cages in a ventilated cabinet with standardized conditions of light (night/day cycle, 12 hours/12 hours) and temperature, and free access to food and water was permitted.

In total, 79 male rats were included in the study. For *in vivo* optical imaging, 65 rats of 3 different ages were examined in this study: 10, 20, and 40 weeks. At each age, SHR were compared with age-matched Wistar Kyoto rats serving as normotensive controls (CTRL). In the 10- and 20-week groups, SHR and CTRL were directly compared. The 40-week group was divided into 4 subgroups: (1) CTRLs, (2) untreated SHR, (3) SHR treated for 10 weeks with losartan, and (4) SHR treated for 10 weeks with verapamil.

Surgical Preparation

All surgical procedures were performed under isoflurane anesthesia (2.5%–3.5%). Catheters were inserted into the right femoral artery and vein. Animals were tracheotomized and artificially ventilated. The skull above the left barrel cortex (1 mm caudal and 3–6 mm lateral from bregma) was carefully thinned to translucency and covered with 2% agarose type III-A (Sigma–Aldrich, Buchs, Switzerland) in Ringer solution (in g/L: NaCl 8.6, CaCl₂ 0.33, KCl 0.30) and a circular glass coverslip. The animals' temperature was kept constant at 37°C. After surgery, isoflurane was discontinued and anesthesia was maintained with an initial subcutaneous injection of α -chloralose (44 mg/kg; Sigma–Aldrich) followed by continuous subcutaneous infusion (22 mg/kg per hour).

Sensory Stimulation

After a baseline of 2 s, a single vibrissa contralateral to the thinned skull was deflected for 4 s at a frequency of 4 Hz.

In Vivo Optical Imaging

Imaging experiments were performed after a postoperative recovery period of at least 1 hour to achieve a stable level of α -chloralose anesthesia and stable imaging signals. Intrinsic optical imaging and laser speckle imaging were acquired following the method previously described by our group¹⁵ (Figure IA–IC in the online-only Data Supplement). Baseline red blood cell (RBC) velocity was determined using 2-photon microscopy (line scan technique¹⁶; Figure ID in the online-only Data Supplement). For this purpose, in 23 animals of the

40-week age groups (CTRL, n=5; SHR, n=5; losartan, n=6; verapamil, n=7) the thinned skull and the dura mater above the activated cortical area were removed after intrinsic optical widefield imaging. After staining the cortex with the fluorescent astrocyte marker sulforhodamine (Sigma–Aldrich) and covering with 2% agarose, 2-photon laser scanning microscopy was performed using a custom-built microscope equipped with a 16 \times objective (0.8 NA; Nikon, Japan).¹⁷ Blood plasma was labeled with a 0.5-mL bolus of 5% fluorescein isothiocyanate–labeled dextran (10 kDa; Sigma–Aldrich). Further details of the imaging methods, including data analysis, are given in the online-only Data Supplement.

Antihypertensive Treatment

Verapamil (80 mg/kg per day)¹⁸ and losartan (30 mg/kg per day)¹⁹ were orally administered to SHR at the age of 30 weeks for a period of 10 weeks. During the treatment period, blood pressure was monitored by regular tail cuff measurements.

Tissue Staining, RNA Isolation, Reverse Transcription, and Quantitative Polymerase Chain Reaction

After functional imaging, rats were deeply anesthetized with pentobarbital (60 mg/kg *i.p.*) and perfused transcardially with ice-cold fixative (0.15 M sodium phosphate buffer, 4% paraformaldehyde, pH 7.4). In some of the 40-week-old animals, Nissl, ionized calcium-binding adaptor molecule 1 (Iba1), and antifibrinogen staining were performed on 40- μ m-thick sections to visualize lateral ventricle sizes, microglia activation, and blood brain barrier leakage, respectively. In a subset of animals, detailed analysis of the microvascular network was performed with the help of fluorescent intravascular fillings. After the perfusion protocol described above, a subgroup of animals was perfused with 1% fluorescein-labeled albumin mixed with 3% porcine skin gelatin (Sigma–Aldrich). After solidification and cryoprotection, 60- μ m sections were cut. In another part of the 20- and 40-week-old animals, RNA expression analysis of brain lysates was performed after imaging experiments to determine RNA expression levels of eNOS, catalase, and the active subunit ncf1 of NADPH. Details on the used methods are provided in the online-only Data Supplement.

Data Analysis

Image analysis was performed using custom-written Matlab routines and the software package PMOD (PMOD Technologies Ltd, Zürich, Switzerland).

Optical Imaging

Data were analyzed as recently reported by our group.¹⁵

Two-Photon Laser Scanning Microscopy

Line scan data were analyzed using the Radon transform approach as described by Drew et al.²⁰

Histological Image Acquisition and Processing

Analysis of cresyl violet staining was performed with MCID software (InterFocus Imaging Ltd, Cambridge, United Kingdom). Immunoperoxidase staining analysis was performed using bright-field microscopy (Zeiss AxioScope) and images acquired with an 8-bit digital color camera (Zeiss AxioCam) controlled by AxioVision 4.5 (Zeiss).

Analysis of Vascular Density

Image processing was performed with Matlab (Mathworks, Natick, MA). The fluorescein isothiocyanate images were filtered, thresholded, and eroded to yield single-pixel-wide traces of the vessels.

Layer-specific regions of interest of the somatosensory cortex were defined manually on the 4',6-diamidino-2-phenylindole images and transferred to the respective vessel trace from the same location. The length density, mean vessel caliber, and volume fraction were then computed stereologically for each cortical layer and the white matter (see Weber et al²¹ for details).

Statistics

Differences between hemodynamic responses between different groups were statistically analyzed using the Mann–Whitney *U* test. Data are presented as mean±SEM.

Results

Mean arterial blood pressure (MAP; mmHg) and heart rate (bpm) were continuously recorded via a femoral catheter during the imaging experiments. The aHTN was already apparent in SHR_s at 10 weeks of age and only slightly more pronounced later (Figure IIA in the online-only Data Supplement). Heart rate was higher in SHR_s than in CTRL only in the 40-week age group (Figure IIB in the online-only Data Supplement). SHR_s aged 20 and 40 weeks had a smaller body weight than age-matched CTRL_s, whereas no weight difference was observed in the 10-week group (Figure IIC in the online-only Data Supplement).

Hemodynamic Responses are Impaired in SHR_s in the 20- and 40-Week Groups

Rats of 10, 20, and 40 weeks of age were imaged by multiwavelength spectroscopy and laser speckle imaging (CTRL, *n*=5, 8, 11 and SHR, *n*=5, 7, 12, respectively) and relative changes in total hemoglobin, cerebral blood volume, and rCBF were measured. Figure 1 shows that in the CTRL group, both cerebral blood volume (Figure 1A) and rCBF (Figure 1B) evoked signals increased with age. The area under the curve and peak response exhibited a significant increase from 10 to 20 weeks and remained high in the 40-week group. In contrast, the time span of the responses was unaltered at all ages (Figure 1C and 1D). When comparing the 10-week CTRL group with the respective age-matched SHR group, we observed very similar hemodynamic responses (peak value and area under the curve), despite the difference in MAP (Figure IIA in the online-only Data Supplement). However, as the SHR_s aged, the evoked responses remained stable until 40 weeks, not displaying any significant changes in time span, amplitude, or area under the curve. Finally, the time span of evoked responses was always slightly but significantly longer in the CTRL group than in the SHR group, already apparent at 10 weeks of age.

Baseline Capillary Red Blood Cell Velocity is Increased in Sustained aHTN

To assess the impact of aHTN and the effects of the losartan and verapamil treatments on baseline microcirculation, we quantified capillary RBC velocity in a subset of the 40-week-old animals (in 23 of 40 animals) using the line scan technique¹⁶ (Figure 1D in the online-only Data Supplement). The 2-photon experiments were conducted on the same animals used for the intrinsic optical imaging experiments and the capillary areas were chosen for recordings in the same cortex area that was previously imaged. RBC velocity in SHR_s measured during resting conditions was higher than in CTRL animals.

Treatment with losartan reduced RBC velocity back to CTRL values, whereas treatment with verapamil reduced RBC velocity without reaching statistical significance (Figure 2B).

Ten-week Treatment With Losartan or Verapamil Does Not Normalize Hemodynamic Responses in SHR_s

Regular tail cuff measurements during the treatment period confirmed the antihypertensive effects of both drugs. The MAP of SHR_s treated with losartan was significantly lowered compared with the MAP of untreated SHR_s and reached the level of the CTRL group at the time of imaging, indicating that the losartan treatment normalized blood pressure values. In the verapamil-treated group, the MAP was significantly lowered compared with the SHR group, but did not reach the level observed in CTRL animals (Figure 2C). Besides this, losartan and verapamil treatment did not alter neither body weight nor heart rate in comparison with untreated SHR_s (Figure III in the online-only Data Supplement).

Despite the reduction in MAP, the stimulation-evoked hemodynamic responses of the losartan and verapamil groups were not significantly different from those observed in untreated SHR_s (Figure 2A1 and 2A2). None of the parameters used to characterize the responses—area under the curve, peak response, and time span—were found to be different when compared with untreated SHR_s (Figure 2A1 and 2A2).

Interestingly, in SHR_s (treated and untreated) the peak hemodynamic responses for both rCBF and cerebral blood volume increased with decreasing MAP values (Figure 2D). In control animals, this association was not found. Although both treatments increased the hemodynamic responses toward control levels, neither of them completely normalized the evoked responses (Figure 2D). In line with the observed extent of reduction in MAP by the 2 drugs (Figure 2C), losartan was observed to be more effective than verapamil in raising the blood flow responses (Figure 2D).

SHR_s Exhibit Brain Atrophy but No Changes in Microvascular Density or Vessel Diameter

Cerebral atrophy was evaluated in all 40-week groups. Compared with CTRL animals, SHR_s exhibited larger lateral ventricles and a thinner cortex in the occipital region (Nissl stained sections; Figure 3A and 3B). Both are signs of progressive cerebral atrophy.²²

Detailed analyses of the microvascular network,²¹ such as volume fraction, length density, and vessel diameters revealed no differences between the subgroups at 40 weeks. In addition, they did not differ from age-matched CTRL animals (Figure 3C).

No Inflammatory Reactions and Blood–Brain Barrier Leakage Occur in the Brains of CTRL_s and SHR_s

Microglial cells form a network of highly responsive surveillance and defense cells,²³ sensitive to pathological changes in the central nervous system. On tissue disturbance, they exhibit morphological adjustments when they move from a resting ramified morphology to an activated state with an

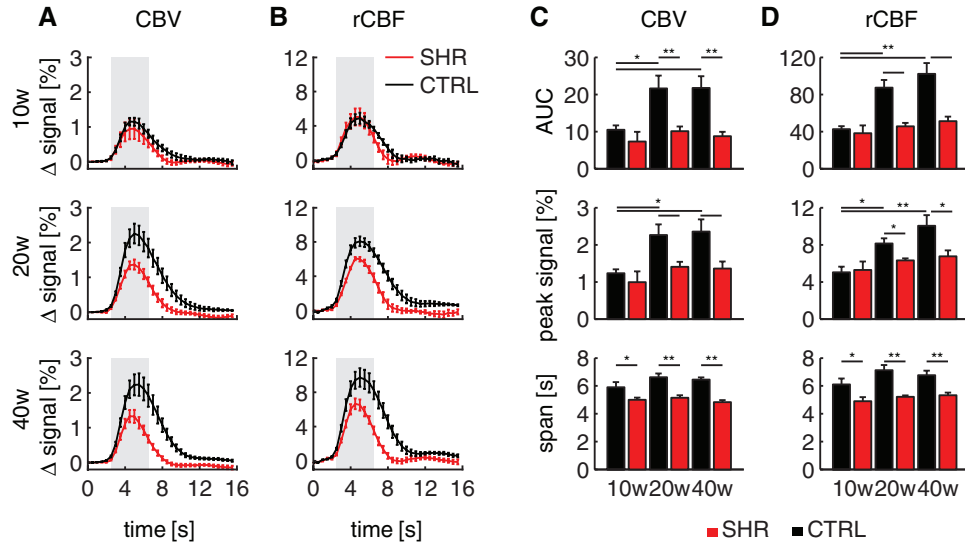


Figure 1. Impairment of the hemodynamic response increases with duration of arterial hypertension. Cerebral blood volume (CBV; **A**) and regional cerebral blood flow (rCBF; **B**) relative signal changes for control (CTRLs; black) and spontaneously hypertensive rat (SHRs; red). Rats were imaged at 10, 20, and 40 weeks of age (CTRL: n=5, 8, 11; SHR: n=5, 7, 12, respectively). Area under the curve (AUC), peak signal, and time span of CBV (**C**) and rCBF (**D**; Mann-Whitney *U* test; **P*<0.05, ***P*<0.005).

amoeboid morphology.²³ The Iba1 is a macrophage-/microglia-specific calcium-binding protein, and it has been shown to be upregulated during inflammation.²⁴ In all 4 groups at 40 weeks of age (CTRL, SHR, losartan, and verapamil), a low baseline Iba1 staining was observed, but no morphological differences were qualitatively identified in Iba1-positive cells. On the basis of this, we concluded that there were no inflammatory changes in the 4 groups of aged 40 weeks (Figure 3A). In

fibrinogen stainings of 40-week-old CTRLs and SHRs, no extravascular fibrinogen deposits and, therefore, no signs of blood-brain barrier leakage could be observed (Figure 3A).

eNOS and Catalase Expression Levels are Increased in Brains of Hypertensive Rats

Expression analyses of brain lysates detected a blood pressure-dependent increase in eNOS expression in 20-week-old rats

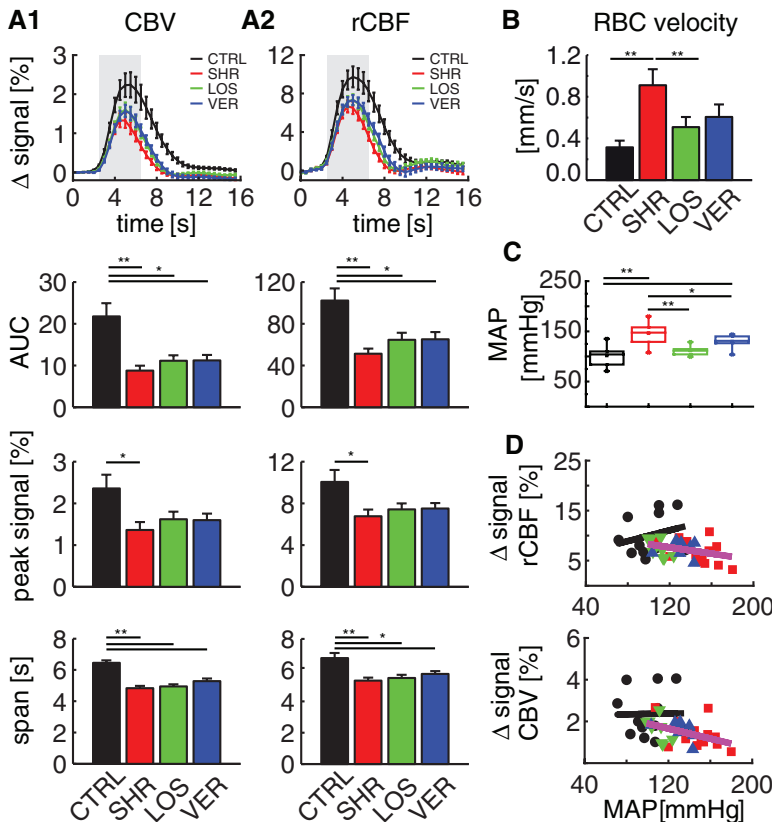


Figure 2. Antihypertensive treatment does not restore hemodynamic responses. **A1** and **A2**, from top to bottom, Average evoked cerebral blood volume (CBV)/regional cerebral blood flow (rCBF) responses and corresponding area under the curve (AUC), peak signal, and time span in the 40-week-old animals (mean±SEM): CTRL group (n=11), spontaneously hypertensive rat (SHR) group (n=12), losartan-treated group (LOS; n=9), and verapamil-treated group (VER; n=8). **B**, Red blood cell (RBC) baseline velocity (mean±SEM) for CTRL (n=17 total capillary segments in all examined animals of this group), SHR (n=12), LOS (n=27), and VER (n=24). **C**, Box plot of mean arterial blood pressure (MAP) values for 40-week-old rats (CTRL, n=14; SHR, n=14; LOS, n=10; VER, n=9); **D**, Correlation between peak rCBF and MAP (top, pink line: *R*=0.451; *P*<0.05) and peak CBV and MAP (bottom, pink line: *R*=0.382; *P*<0.05) in all hypertensive groups (SHR, LOS, and VER). In both cases, no significant correlation was observed to MAP for the CTRL group (black lines; Mann-Whitney *U* test. **P*<0.05, ***P*<0.005).

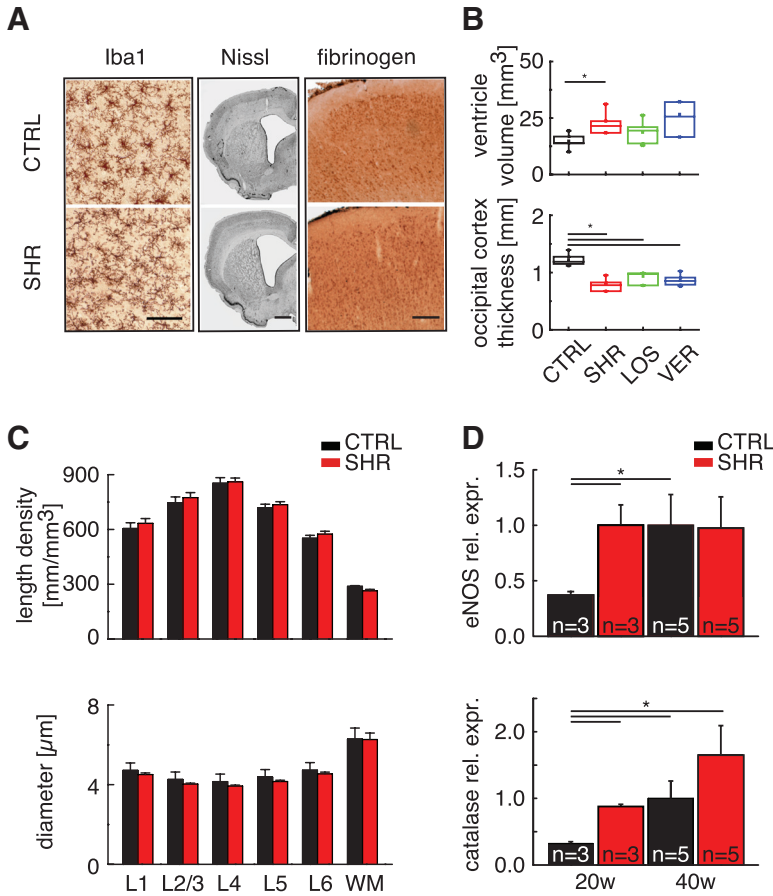


Figure 3. Structural and biochemical analyses reveal brain atrophy in 40-week-old spontaneously hypertensive rats (SHRs) without active inflammatory reactions and increased antioxidant defense. **A**, Iba1 (left; scale bar 100 μm), Nissl (middle; scale bar 1 mm), and fibrinogen staining (right; scale bar 200 μm) from controls (CTRLs) and SHRs. Four brains from every group at 40 weeks of age (CTRL, SHR, losartan-treated group [LOS], verapamil-treated group [VER]) were stained for ionized calcium-binding adaptor molecule 1 (Iba1) and 4 brains of CTRL and SHR animals for fibrinogen. **B**, Box plots of lateral ventricle volumes (mm³, top) and occipital cortex thickness (mm, bottom) of 40-week-old rats: CTRL (n=5), SHR (n=4), LOS (n=4), and VER (n=5; Mann-Whitney *U* test; **P*<0.05). **C**, Layer-specific microvascular analysis of the barrel cortex: capillary length density (mm/mm³, top) and diameter (mm, bottom) are reported as mean±SEM (CTRL n=3, SHR n=5; WM=white matter). **D**, Expression analyses derived from lysates of the somatosensory cortices of 20- and 40-week-old rats were assessed by real-time polymerase chain reaction: eNOS (top) and catalase (bottom; the following number of animals was examined: 20w CTRL: n=3, 20w SHR: n=3, 40w CTRL: n=5, 40w SHR: n=5).

(Figure 3D) in individual experiments (n=3 for both CTRLs and for SHRs), suggesting impaired endothelial homeostasis. Single experiments reproducibly showed increased expression levels in 40-week-old animals (n=5) compared with 20-week-old CTRL rats (n=3) and did not differ between hypertensive and normotensive animals at 40 weeks of age. Moreover, we observed an age- and blood pressure-dependent increase in cerebral catalase expression, suggesting enhanced oxidative stress in both aging and sustained hypertension (Figure 3D). A trend toward a blood pressure-dependent increase in the active subunit of NADPH oxidase from 1.08±0.21 to 1.43±0.24 (40-week CTRL versus 40-week SHR; n=5 for each group; *P*=0.31; Figure IV in the online-only Data Supplement) may contribute to increased generation of reactive oxygen species (ROS) in sustained hypertension.

Discussion

aHTN constitutes a major risk factor for transient ischemic attacks and stroke. Several studies have investigated the role of aHTN in the pathogenesis of stroke²⁵ and assessed the benefits of lowering elevated blood pressure for stroke prevention. Less is known about the impact of aHTN on physiological CBF-related processes, such as NVC.

Our results indicate that aHTN alone does not explain the impaired neurovascular response. Although increased MAP was already present in 10-week-old SHRs (Figure IIA in the online-only Data Supplement), the cerebrovascular dysfunction only became evident at the age of 20 weeks and later

(Figure 1). The increased blood pressure in the early phase of aHTN may be compensated by the brain through auto-regulation²⁶ and is not sufficient to induce the observed functional disturbances in rCBF. Functional impairment was only detected at a later stage, presumably after the permanent interference of hypertension exceeded compensatory responses. Biochemical and structural changes triggered by sustained hypertension may induce a dysfunction in NVC. Higher blood velocity associated with aHTN leads to increased shear stress on the blood vessel wall, which has been reported to result in the remodeling of cellular and extracellular components in the vessel wall.²⁷

In addition, we observed a marked increase in baseline RBC velocity in SHRs (40 weeks) compared with normotensive control animals. This finding seems to be in contrast to the findings of other studies showing maintained^{4,11} or decreased CBF.²⁸ However, our study is the first one to selectively investigate the relationship between blood pressure and CBF at the capillary level. Taking capillary RBC velocity as a surrogate marker for the resting CBF, this may partially explain the impaired evoked rCBF responses in SHRs. The increased resting CBF augments oxygen and energy substrate supply at baseline. As a consequence, a smaller change in rCBF on stimulation could suffice to meet the metabolic needs during increased neuronal activity.

We observed an increase of relative signal changes over time in control animals. Unfortunately, we do not have data from younger animals on the absolute baseline blood flow.

However, baseline blood flow seems to be one of the main determinants of the rCBF response.²⁹ For baseline blood flow, changes in both directions have been observed in older subjects.^{13,30,31} There is also no agreement in the literature about the development of the hemodynamic response with age. There are reports demonstrating decreasing^{14,32} and increasing (as in our study) responses.¹³ This may depend on species, anesthesia, stimulation type, and applied imaging methods.

The close similarity between MAP and RBC velocity (compare Figure 2B and 2C) suggests a direct relationship between increased arteriovenous pressure gradient and blood flow velocity. For such a direct relationship to be true, 2 prerequisites must be fulfilled: (1) impaired cerebral autoregulation and (2) unaltered microvascular density (see below).

Intact cerebral autoregulation maintains a constant perfusion of brain parenchyma within a certain blood pressure range and depends on various mechanisms, such as myogenic, neurogenic/sympathetic, and endothelial components.³³ In sustained aHTN, cerebral autoregulation is altered mainly because of vascular hypertrophy.³⁴ The reduced hemodynamic response on activation observed in 20- and 40-week-old SHR animals points to an impaired capacity of precapillary vessels to dilate.

From a fluid dynamics perspective, blood flow velocity depends on the resistance and the pressure gradient between 2 compartments. As stated above, the increased pressure gradient is likely a major cause for the augmented RBC velocity in 40-week SHR animals. Antihypertensive treatment with both drugs decreased MAP values and therewith reduced the pressure gradient, thus leading to a normalization of baseline capillary blood flow. Nevertheless, changes in the pressure gradient alone are not sufficient to explain the observed functional hemodynamic changes. Indeed, 10 weeks of treatment with the angiotensin II type 1 receptor antagonist losartan or with the calcium channel blocker verapamil were not sufficient to normalize hemodynamic responses (Figure 2) and to reverse increased oxidative stress, endothelial imbalance, and brain atrophy. The fact that the medical treatment led to a shift of the hemodynamic responses toward control levels (Figure 2D) but was not able to completely normalize aHTN-induced changes further supports the notion that additional factors are involved in the development of disturbed blood flow responses. The exact reasons for the incomplete recovery after treatment remain unclear. Insufficient treatment duration and suboptimal dosage could be important factors; however, treatment durations as short as 4 weeks and lower drug doses have been reported to be effective to reverse structural changes for both losartan³⁵ and verapamil.³⁶

More importantly, a single pharmacological target might not be sufficient. Indeed, Dupuis et al³⁷ recently reported that telmisartan—an angiotensin II type 1 receptor antagonist like losartan—does not have a significant impact on mean cerebral arteriolar pressure in SHR animals.

Apart from inducing structural changes, aHTN alters molecular mechanisms critical for functional integrity of the neurovascular unit at both the neural and the vascular level. aHTN is known to favor an imbalance in antioxidant defense systems and a disruption of endothelial homeostasis.^{38,39} Capone et al⁴⁰ demonstrated that ROS production in the subfornical organ is

involved in the NVC impairment observed in aHTN. Similar events may be reflected in our expression analysis of cerebral lysates in which we observed a trend toward increased expression levels of the cytosolic active subunit of NADPH oxidase, an important source of ROS in endothelial cells. Increased levels of catalase, an enzyme scavenging free radicals, suggest a blood pressure-dependent and age-dependent enhancement of this antioxidative defense mechanism. Therefore, increased generation of ROS on aging and sustained hypertension may exceed the cerebral antioxidant defense capacity, and thereby contribute to cerebral endothelial and vascular dysfunction, as suggested by others.^{41–44}

A key mechanism by which intact endothelial cells communicate with the underlying vascular smooth muscle cells constitutes eNOS-derived nitric oxide.^{45,46} Endothelial (and neuronal) cell-mediated nitric oxide-dependent vascular relaxation is known to contribute to increased CBF. We found increased levels of eNOS in 20-week-old hypertensive animals; this may reflect a compensatory mechanism in response to reduced CBF, in accordance with earlier reports describing an upregulation of cerebral eNOS in SHR animals.⁴⁷ A similar compensatory increase in eNOS has been described in rats on aging. Van der Loo et al⁴⁸ found an increase in O₂⁻, trapping of vasorelaxant nitric oxide, and subsequent peroxynitrite formation, followed by nitration and inhibition of manganese superoxide dismutase.

Taken together, our findings support the notion that insufficient compensation for increased cerebral levels of ROS and impaired endothelial homeostasis contribute to impaired NVC.

The spectrum of different reported findings reflects the complex nature of cerebrovascular regulation in the pathophysiology of essential aHTN and underlines the need for further *in vivo* research using multimodal imaging technology.

Limitations

The use of older animals may allow the effects of sustained aHTN and aging on CBF to be addressed specifically. For technical reasons, our 2-photon imaging of capillary RBC velocity was limited to 40-week-old animals and only included resting state measurements. The number of animals used for expression analyses and histology is low and as a consequence small effects might remain undetected. Concerning the microvascular analysis, our histological measurements incompletely reflect the physiological *in vivo* situation, mainly because of a lack of vascular tone and intraluminal pressure. In addition, our histological approach measuring the vascular network has a spatial resolution of 0.7 μm²¹ and as a consequence small differences might remain undetected. But our results were in accordance with other groups that have not found consistent differences between SHR and CTRL animals in the cerebral capillary network⁴⁹ and in arterial luminal diameter.⁵⁰ It has to be noted here that we did not examine other signs of vasculopathologies, such as vessel wall thickening, stenosis, or local thrombosis, which could contribute to the impaired autoregulation.

All histological examinations performed in the present study (brain atrophy, inflammatory reactions, etc) were only

done in 40-week-old animals. However, predictions about the development of these morphological changes over time would require measures in younger animals as well. Thus, our data do not allow us to conclude whether drug treatment can prevent structural changes, such as cortical thinning.

Finally, one should remain cautious when comparing imaging data (Figures 1 and 2) with expression analyses of brain lysates (eg, eNOS and catalase expression levels in Figure 3D and Figure IV in the online-only Data Supplement). With regard to imaging data, the 2-photon measurement is a pure capillary readout. Similarly, laser speckle imaging performed at the chosen integration time (10 ms) mainly probes microvessels, as it cannot resolve the temporal dynamics of larger vessels with higher blood velocity. However, the brain lysates used for expression analyses will contain a majority of microvessels, but by nature of a tissue lysate, contain all vessel sizes.

Conclusions

Increased duration of aHTN in rats led to a progressive impairment of the hemodynamic responses after sensory stimulation and to an elevated baseline capillary RBC velocity. Monotherapy of hypertension was not insufficient to normalize impaired hemodynamic response. Our findings highlight the need for refined treatment strategies to address cerebrovascular dysfunction in sustained hypertension. Additional research is required to elucidate possible interactions between sustained aHTN and aging. This will be of particular interest for therapeutic efforts aimed at inhibiting the progression of neurodegenerative diseases, such as Alzheimer disease or vascular dementia or preventing the development of stroke, where the pathophysiology involves impaired blood supply.⁵¹

Disclosures

The authors are grateful for the support of the University Research Priority Program Integrative Human Physiology at the University of Zurich (to Drs Calcinaghi, Buck, Matter, and Weber), the Swiss National Science Foundation (PP00B-110751/1 to Dr Weber, 31003A-124739/1 to Dr Wyss, and 310030-130626/1 to Dr Matter) and the EMDO, Hartmann Müller, and Olga Mayenfisch foundations (to Dr Jolivet). Dr Jolivet is supported by a Marie Curie fellowship.

References

- Lawes CM, Vander Hoorn S, Rodgers A; International Society of Hypertension. Global burden of blood-pressure-related disease, 2001. *Lancet*. 2008;371:1513–1518.
- Goldstein LB, Adams R, Alberts MJ, Appel LJ, Brass LM, Bushnell CD, et al. Primary prevention of ischemic stroke: A guideline from the American heart association/American stroke association stroke council: Cosponsored by the atherosclerotic peripheral vascular disease interdisciplinary working group; cardiovascular nursing council; clinical cardiology council; nutrition, physical activity, and metabolism council; and the quality of care and outcomes research interdisciplinary working group: The American academy of neurology affirms the value of this guideline. *Stroke*. 2006;37:1583–1633
- Dahlöf B. Prevention of stroke in patients with hypertension. *Am J Cardiol*. 2007;100(3A):17J–24J.
- Wei L, Lin SZ, Tajima A, Nakata H, Acuff V, Patlak C, et al. Cerebral glucose utilization and blood flow in adult spontaneously hypertensive rats. *Hypertension*. 1992;20:501–510.
- Leoni RF, Paiva FF, Henning EC, Nascimento GC, Tannús A, de Araujo DB, et al. Magnetic resonance imaging quantification of regional cerebral blood flow and cerebrovascular reactivity to carbon dioxide in normotensive and hypertensive rats. *Neuroimage*. 2011;58:75–81.
- Katsuta T. Decreased local cerebral blood flow in young and aged spontaneously hypertensive rats. *Fukuoka Igaku Zasshi*. 1997;88:65–74.
- Heinert G, Casadei B, Paterson DJ. Hypercapnic cerebral blood flow in spontaneously hypertensive rats. *J Hypertens*. 1998;16:1491–1498.
- Kazama K, Anrather J, Zhou P, Girouard H, Frys K, Milner TA, et al. Angiotensin II impairs neurovascular coupling in neocortex through NADPH oxidase-derived radicals. *Circ Res*. 2004;95:1019–1026.
- Capone C, Faraco G, Anrather J, Zhou P, Iadecola C. Cyclooxygenase 1-derived prostaglandin E2 and EP1 receptors are required for the cerebrovascular dysfunction induced by angiotensin II. *Hypertension*. 2010;55:911–917.
- Iadecola C, Capone C, Faraco G, Park L, Cao XA, Davisson RL. The cerebrovascular dysfunction induced by slow pressor doses of angiotensin II precedes the development of hypertension. *Am J Physiol-Heart Circ Physiol*. 2011;300:H397–H407
- Jennings JR, Muldoon MF, Ryan C, Price JC, Greer P, Sutton-Tyrrell K, et al. Reduced cerebral blood flow response and compensation among patients with untreated hypertension. *Neurology*. 2005;64:1358–1365.
- Bentourkia M, Bol A, Ivanoiu A, Labar D, Sibomana M, Coppens A, et al. Comparison of regional cerebral blood flow and glucose metabolism in the normal brain: effect of aging. *J Neurol Sci*. 2000;181:19–28.
- Ances BM, Liang CL, Leontiev O, Perthen JE, Fleisher AS, Lansing AE, et al. Effects of aging on cerebral blood flow, oxygen metabolism, and blood oxygenation level dependent responses to visual stimulation. *Hum Brain Mapp*. 2009;30:1120–1132.
- Dubeau S, Ferland G, Gaudreau P, Beaumont E, Lesage F. Cerebrovascular hemodynamic correlates of aging in the Lou/c rat: a model of healthy aging. *Neuroimage*. 2011;56:1892–1901.
- Calcinaghi N, Jolivet R, Wyss MT, Ametamey SM, Gasparini F, Buck A, et al. Metabotropic glutamate receptor mGluR5 is not involved in the early hemodynamic response. *J Cereb Blood Flow Metab*. 2011;31:e1–10.
- Kleinfeld D, Mitra PP, Helmchen F, Denk W. Fluctuations and stimulus-induced changes in blood flow observed in individual capillaries in layers 2 through 4 of rat neocortex. *Proc Natl Acad Sci USA*. 1998;95:15741–15746.
- Haiss F, Jolivet R, Wyss MT, Reichold J, Braham NB, Scheffold F, et al. Improved *in vivo* two-photon imaging after blood replacement by perfluorocarbon. *J Physiol*. 2009;587(Pt 13):3153–3158.
- Fortepiani LA, Rodrigo E, Ortíz MC, Cachofeiro V, Atucha NM, Ruilope LM, et al. Pressure natriuresis in nitric oxide-deficient hypertensive rats: effect of antihypertensive treatments. *J Am Soc Nephrol*. 1999;10:21–27.
- Gohlke P, Linz W, Schölkens BA, Wiemer G, Unger T. Cardiac and vascular effects of long-term losartan treatment in stroke-prone spontaneously hypertensive rats. *Hypertension*. 1996;28:397–402.
- Drew PJ, Blinder P, Cauwenberghs G, Shih AY, Kleinfeld D. Rapid determination of particle velocity from space-time images using the Radon transform. *J Comput Neurosci*. 2010;29:5–11.
- Weber B, Keller AL, Reichold J, Logothetis NK. The microvascular system of the striate and extrastriate visual cortex of the macaque. *Cereb Cortex*. 2008;18:2318–2330.
- Amenta F, Antonietta M, Tullio D, Tomassoni D. Arterial hypertension and brain damage—evidence from animal models (review). *Clin Exp Hyperts*. 2003;25:359–380
- Kettenmann H, Hanisch UK, Noda M, Verkhratsky A. Physiology of microglia. *Physiol Rev*. 2011;91:461–553.
- Imai Y, Kohsaka S. Intracellular signaling in M-CSF-induced microglia activation: role of Iba1. *Glia*. 2002;40:164–174.
- Sacco RL. Newer risk factors for stroke. *Neurology*. 2001;57(5 Suppl 2):S31–S34.
- Claassen JA, van Beek AH, Rikkert MG, Jansen RW. Cerebral autoregulation: An overview of current concepts and methodology with special focus on the elderly. *J Cereb Blood Flow Metab*. 2008;28:1071–1085
- Baumbach GL, Heistad DD. Adaptive changes in cerebral blood vessels during chronic hypertension. *J Hypertens*. 1991;9:987–991.
- Beason-Held LL, Moghekar A, Zonderman AB, Kraut MA, Resnick SM. Longitudinal changes in cerebral blood flow in the older hypertensive brain. *Stroke*. 2007;38:1766–1773.
- Franceschini MA, Radhakrishnan H, Thakur K, Wu W, Ruvinskaya S, Carp S, et al. The effect of different anesthetics on neurovascular coupling. *Neuroimage*. 2010;51:1367–1377.
- Aanerud J, Borghammer P, Chakravarty MM, Vang K, Rodell AB, Jónsdóttir KY, et al. Brain energy metabolism and blood flow differences in healthy aging. *J Cereb Blood Flow Metab*. 2012;32:1177–1187.

31. Yao H, Ooboshi H, Ibayashi S, Uchimura H, Fujishima M. Cerebral blood flow and ischemia-induced neurotransmitter release in the striatum of aged spontaneously hypertensive rats. *Stroke*. 1993;24:577–580.
32. Park L, Anrather J, Girouard H, Zhou P, Iadecola C. Nox2-derived reactive oxygen species mediate neurovascular dysregulation in the aging mouse brain. *J Cereb Blood Flow Metab*. 2007;27:1908–1918.
33. Ohta K, Gotoh F, Shimazu K, Amano T, Komatsumoto S, Hamada J, et al. Locus coeruleus stimulation exerts different influences on the dynamic changes of cerebral pial and intraparenchymal vessels. *Neurol Res*. 1991;13:164–167.
34. Paulson OB, Strandgaard S, Edvinsson L. Cerebral autoregulation. *Cerebrovasc Brain Metab Rev*. 1990;2:161–192.
35. Sabino B, Lessa MA, Nascimento AR, Rodrigues CA, Henriques Md, Garzoni LR, et al. Effects of antihypertensive drugs on capillary rarefaction in spontaneously hypertensive rats: intravital microscopy and histologic analysis. *J Cardiovasc Pharmacol*. 2008;51:402–409.
36. Vaja V, Ochodnický P, Kreněk P, Klimas J, Bajuszova Z, Kyselovic J. Rapid large artery remodeling following the administration and withdrawal of calcium channel blockers in spontaneously hypertensive rats. *Eur J Pharmacol*. 2009;619:85–91.
37. Dupuis F, Vincent JM, Limiñana P, Chillon JM, Capdeville-Atkinson C, Atkinson J. Effects of suboptimal doses of the AT1 receptor blocker, telmisartan, with the angiotensin-converting enzyme inhibitor, ramipril, on cerebral arterioles in spontaneously hypertensive rat. *J Hypertens*. 2010;28:1566–1573.
38. Chrissobolis S, Faraci FM. The role of oxidative stress and NADPH oxidase in cerebrovascular disease. *Trends Mol Med*. 2008;14:495–502.
39. Girouard H, Park L, Anrather J, Zhou P, Iadecola C. Cerebrovascular nitrosative stress mediates neurovascular and endothelial dysfunction induced by angiotensin II. *Arterioscler Thromb Vasc Biol*. 2007;27:303–309.
40. Capone C, Faraco G, Peterson JR, Coleman C, Anrather J, Milner TA, et al. Central cardiovascular circuits contribute to the neurovascular dysfunction in angiotensin II hypertension. *J Neurosci*. 2012;32:4878–4886.
41. Girouard H, Park L, Anrather J, Zhou P, Iadecola C. Angiotensin II attenuates endothelium-dependent responses in the cerebral microcirculation through nox-2-derived radicals. *Arterioscler Thromb Vasc Biol*. 2006;26:826–832.
42. Paravicini TM, Chrissobolis S, Drummond GR, Sobey CG. Increased NADPH-oxidase activity and Nox4 expression during chronic hypertension is associated with enhanced cerebral vasodilatation to NADPH in vivo. *Stroke*. 2004;35:584–589.
43. Wang D, Chabrashvili T, Wilcox CS. Enhanced contractility of renal afferent arterioles from angiotensin-infused rabbits: roles of oxidative stress, thromboxane prostanoid receptors, and endothelium. *Circ Res*. 2004;94:1436–1442.
44. Weber DS, Rocic P, Mellis AM, Laude K, Lyle AN, Harrison DG, et al. Angiotensin II-induced hypertrophy is potentiated in mice overexpressing p22phox in vascular smooth muscle. *Am J Physiol Heart Circ Physiol*. 2005;288:H37–H42.
45. Faraci FM. Protecting the brain with eNOS: run for your life. *Circ Res*. 2006;99:1029–1030.
46. Toda N, Ayajiki K, Okamura T. Cerebral blood flow regulation by nitric oxide: recent advances. *Pharmacol Rev*. 2009;61:62–97.
47. Hojná S, Kadlecová M, Dobesová Z, Valousková V, Zicha J, Kunes J. The participation of brain NO synthase in blood pressure control of adult spontaneously hypertensive rats. *Mol Cell Biochem*. 2007;297:21–29.
48. van der Loo B, Labugger R, Skepper JN, Bachschmid M, Kilo J, Powell JM, et al. Enhanced peroxynitrite formation is associated with vascular aging. *J Exp Med*. 2000;192:1731–1744.
49. Lin SZ, Sposito N, Pettersen S, Rybacki L, McKenna E, Pettigrew K, et al. Cerebral capillary bed structure of normotensive and chronically hypertensive rats. *Microvasc Res*. 1990;40:341–357.
50. Struijker Boudier HA, le Noble JL, Messing MW, Huijberts MS, le Noble FA, van Essen H. The microcirculation and hypertension. *J Hypertens Suppl*. 1992;10:S147–S156.
51. Iadecola C, Davisson RL. Hypertension and cerebrovascular dysfunction. *Cell Metab*. 2008;7:476–484.